proceedings

MDPI

Proceedings

Accurate Measurement of Stress Distribution Using $NaNbO_3$:Pr Microparticles †

Xiangli Li [1], Xiaorui Han [2] and Guanying Chen [3,*]

* Correspondence: chenguanying@hit.edu.cn

† Presented at the 2nd International Online-Conference on Nanomaterials, 15–30 November 2020; Available online: https://iocn2020.sciforum.net/.

Published: 15 November 2020

Abstract: Dynamic stress/strain imaging is very important for engineering research, but there is no strain sensor for onsite real-time monitoring. Mechanoluminescent materials have characteristics of light emission induced by mechanical stimulation, which have attracted wide attention. In order to realize the real-time monitoring of stress/strain distribution, a new material synthesis strategy was designed to prepare mechanical luminescent materials. All experimental results show that this material can be applied to stress/strain distribution detection. This new type of mechanoluminescent material is expected to usher in a new era of high resolution strain imaging and contribute to the research of precise dynamic stress/strain imaging of structures.

Keywords: Mechanoluminescence; stress distribution; sensor

1. Introduction

Mechanoluminescence (ML) is a kind of luminescent phenomena that produces photon emission by mechanical stimulation [1–4]. Benefiting from the characteristics of linear, repeatability and nondestructive [5], ML materials have attracted more and more attention because of their widely potential applications in the fields of building structural health diagnosis [6–8] and stress distribution imaging [9–11]. How to improve the spatial resolution of materials is a very important topic. There are usually two types of strategies. Firstly, developing new ML phosphors with stronger ML intensity. The luminance of the ML materials depends on the amplitude and nature of the mechanical stimulus. The luminance of some ML materials reported in the literature is shown as follows: ZnS:Cu (83.3–125.5 cd m^{-2}) [12], CaZnOS:Mn^{2+} (30–40 mcd m^{-2}) [13], and $mCaO{\cdot}Nb_2O_5$:Pr^{3+} (m = 1, 2 and 3) (3–35 mcd m^{-2}) [14]. So far, the brightest commercial ML material is $SrAl_2O_4$:Eu^{2+}. Secondly, preparing evenly distributed ML microparticles. The smaller the particle size is, the higher the spatial resolution it has. Due to the large specific surface area of the microparticle, there are many surface defects, which seriously impaire its luminescence [15]. At the same time, the contact area between ML microparticles and polymers becomes larger, which improves the sensitivity of ML [16].

In this study, we prepared the precursor through hydrothermal synthesis, and then the ML material was obtained by high-temperature annealing treatment. By adjusting the doping amount of Pr^{3+}, we obtained a kind of high-brightness nanoscale ML material, $NaNbO_3$:Pr. The ML microparticles and PDMS were combined to prepare the film, and then the stress was applied on the film. According to the luminescence distribution of the film, the stress distribution of the film was successfully detected.

2. Materials and Methods

$NaNbO_3$:Pr microparticles were prepared by hydrothermal method and high temperature annealing treatment. The starting materials were Nb_2O_5 (99.99%), NaOH (99.9%) and Pr_2O_3 (99.99%).

The detailed experimental procedure is listed below. First, Nb_2O_5 and Pr_2O_3 were thoroughly dispersed in sodium hydroxide aqueous solution (25 mL) for 180 min by magnetic stirring, and then transferred to a polytetrafluoroethylene lined autoclaved kettle. After reaction for 6 h at 200 °C, the reaction products were separated and washed with ionized water until neutral, and then dried for 12 h at 60 °C. After that, the precursor was put into a 25 mL alumina crucible, which was filled with activated carbon particles and placed in a large crucible with a lid. Then, the crucible was transferred to muffle furnace and reacted at 1050 °C for 4 h. After cooling to room temperature, the $NaNbO_3$: Pr material was obtained. The $NaNbO_3$: Pr material and PDMS were prepared into a composite film (≈2 mm) at a mass ratio of 1:3 and then cooled in a 0.25 * 0.25 cm grinding tool. In the further analysis, ultraviolet lamp with wavelength of 365 nm was used for irradiation for 1 min.

XRD patterns were collected on X-ray diffractometer (Cu Kα). Surface morphology was characterized by a field-emission SEM. Spectrofluorometer equipped with a 150 W Xe lamp was used for photoluminescence (PL) and photoluminescence excitation (PLE) spectra measurement at room temperature. The ML images were recorded by a high speed charge-coupled device (CCD) camera.

3. Result and Discussion

As shown in Figure 1a, the XRD results show that the prepared sample was pure $NaNbO_3$, which is consistent with the theoretical pattern (Icsd no.: 33-1270). This crystal structure has an orthorhombic asymmetry with a space group Pbma. After doping Pr ions, the refined peaks near 32.5° shift to the higher-angle side indicating a lattice shrinkage induced by the smaller-size Pr ions occupy the Na ions sites in the $NaNbO_3$ host. Figure 1b show SEM images of $NaNbO_3$: Pr, these particles are similar in shape to vertical cubes and range in size from 100 to 350 nm. These results show that our synthetic method can obtain high quality luminescent particles.

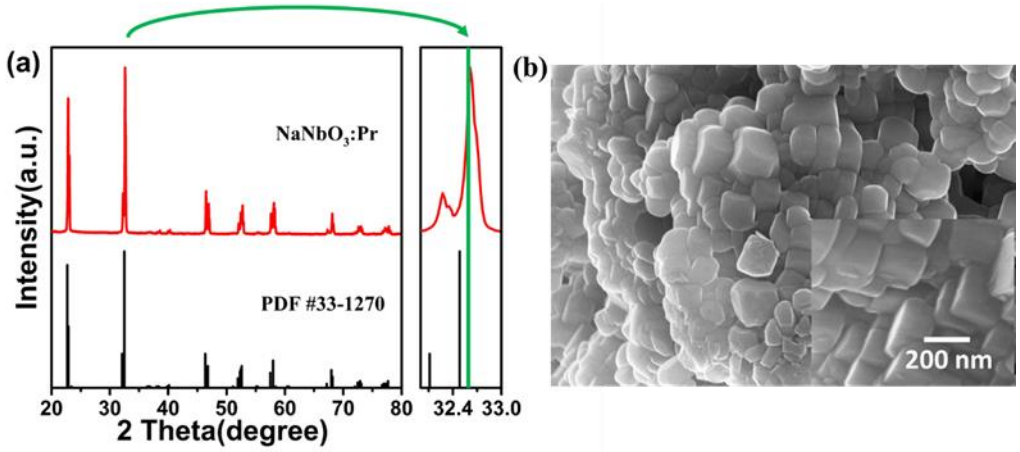

Figure 1. Structural characterization and morphological. (**a**) XRD patterns of the $NaNbO_3$:Pr particles. (**b**) SEM photograph of $NaNbO_3$: Pr.

The ultraviolet-visible diffuse reflection spectrum of $NaNbO_3$:Pr samples are shown in Figure 2a. The sample exhibits high reflectivity in the wavelength range of 500~700 nm. The absorption in the wavelength range of 350~400 nm belongs to the absorption of matrix materials. In order to obtain the optical band gap of $NaNbO_3$:Pr, Kubelka-Munk formula (Formula (1)) was used to calculate the reflection spectrum:

$$F(R) = K/S = (1 - R)^2/(2R) \quad (1)$$

where K, S and R represent the absorption, scattering coefficients and reflection, respectively [17]. The optical band gap of $NaNbO_3$:Pr material was calculated to be 3.25 eV on the basis of derived from Kubelka-Munk equation.

The excitation spectrum (λem = 611 nm) and emission spectrum (λex = 340 nm) of $NaNbO_3$: Pr materials are shown in Figure 2b. The excitation spectrum extends to a wide range and is consistent

with the diffuse reflectance spectrum. The strong excitation band in the wavelength range of 275 nm to 350 nm should attribute to the main lattice absorption. There is a strong main excitation band in the excitation spectrum, indicating that there is an effective energy transfer between $NaNbO_3$ and Pr ions. Three weak excitations with maximum values at 435~450 nm can be attributed to the $^1D_2$-$^3P_{2,1,0}$ electron transition of Pr ions. Under the excitation of 330 nm, the sample showed a red characteristic emission band of Pr ions, with the peak value at 611 nm. This dominant red emission was attributed to the $^1D_2$-$^3H_4$ transition of Pr ions.

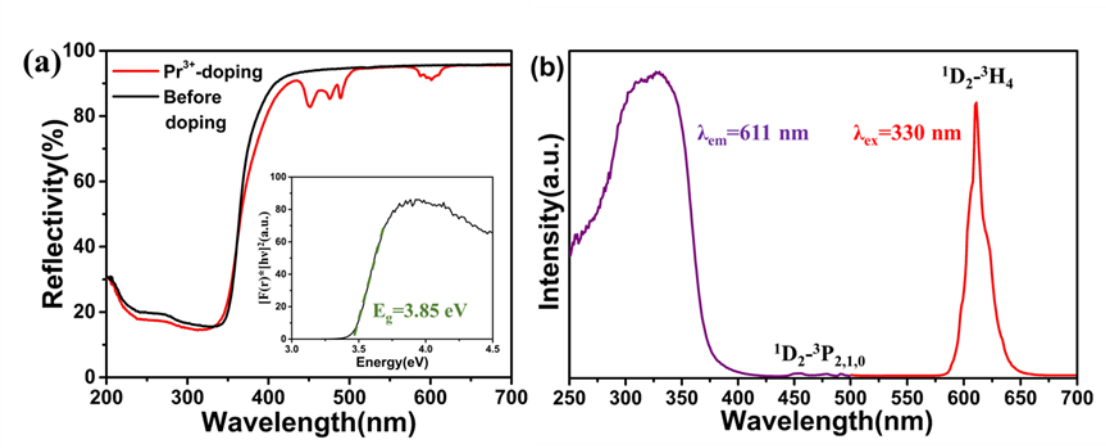

Figure 2. (**a**) Diffuse reflection spectra of the as-synthesized $NaNbO_3$ before and after the Pr ions doping. The inset shows the calculated curve of $(\alpha h\nu)^2$ vs. $h\nu$ by using the Kubelka-Munk function. (**b**) Spectra of PL and PLE of $NaNbO_3$:Pr (λem = 611 nm, λex = 330 nm).

Figure 3 is a real time ML image of friction across the $NaNbO_3$:Pr film recorded by a high-speed CCD camera. After subtracting the background signal from the original ML strength image, the stress distribution on the film can be calculated after conversion. The above results show that $NaNbO_3$:Pr ML film is a very effective material to detect the stress distribution of objects.

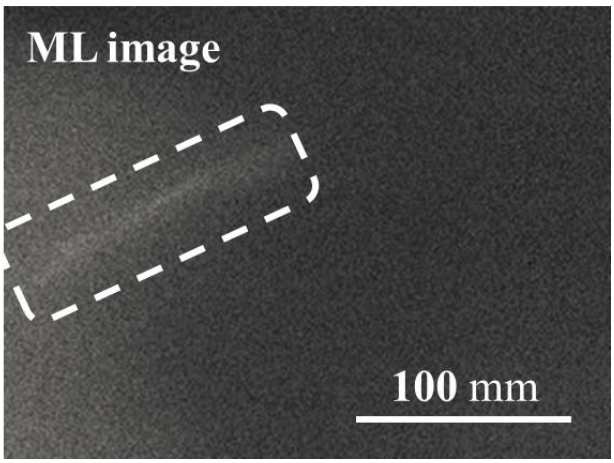

Figure 3. Dynamic imaging of ML.

4. Conclusions

In this paper, $NaNbO_3$:Pr microparticles with size distribution between 100 and 350 nm were prepared using hydrothermal synthesis and high-temperature annealing treatment. We use the obtained $NaNbO_3$:Pr film for dynamic ML imaging. The results show that the $NaNbO_3$:Pr micromaterial is a potential material in sensing and imaging fields.

References

1. Xu, C.-N.; Watanabe, T.; Akiyama, M.; Zheng, X.-G. Direct view of stress distribution in solid by mechanoluminescence. *Appl. Phys. Lett.* **1999**, *74*, 2414–2416.
2. Wiedemann, F.; Schmide, G.C. Ueber luminescenz. *Ann. Phys. Chem.* **1895**, *54*, 604–625.
3. Walton, A.J. Triboluminescence. *Adv. Phys.* **1977**, *26*, 887–948.
4. Tu, D.; Hamabe, R.; Xu, C.-N. Sustainable Mechanoluminescence by Designing a Novel Pinning Trap in Crystals. *J. Phys. Chem. C* **2018**, *122*, 23307–23311.
5. Zhang, J.-C.; Wang, X.; Marriott, G.; Xu, C.-N. Trap-controlled mechanoluminescent materials. *Prog. Mater. Sci.* **2019**, *103*, 678–742.
6. Liu, L.; Xu, C.-N.; Yoshida, A.; Tu, D.; Ueno, N.; Kainuma, S. Scalable Elasticoluminescent Strain Sensor for Precise Dynamic Stress Imaging and Onsite Infrastructure Diagnosis. *Adv. Mater. Technol.* **2018**, *4*, 1800336.
7. Terasaki, N.; Xu, C.-N. Historical-Log Recording System for Crack Opening and Growth Based on Mechanoluminescent Flexible Sensor. *IEEE Sens. J.* **2013**, *13*, 3999–4004.
8. Fujio, Y.; Xu, C.-N.; Terasawa, Y.; Sakata, Y.; Yamabe, J.; Ueno, N.; Terasaki, N.; Yoshida, A.; Watanabe, S.; Murakami, Y. Sheet sensor using $SrAl_2O^4$:Eu mechanoluminescent material for visualizing inner crack of high-pressure hydrogen vessel. *Int. J. Hydrogen Energy* **2016**, *41*, 1333–1340.
9. Li, H.; Zhang, Y.; Dai, H.; Tong, W.; Zhou, Y.; Zhao, J.; An, Q. A self-powered porous ZnS/PVDF-HFP mechanoluminescent composite film that converts human movement into eye-readable light. *Nanoscale* **2018**, *10*, 5489–5495.
10. Li, C.; Xu, C.N.; Zhang, L.; Yamada, H.; Imai, Y. Dynamic visualization of stress distribution on metal by mechanoluminescence images. *J. Vis.* **2008**, *11*, 329–335.
11. Tadesse, Y.; Priya, S.; Stephanou, H; Popa, D.; Hanson, D. Piezoelectric actuation and sensing for facial robotics. *Ferroelectrics* **2006**, *345*, 13–25.
12. Jeong, S.-M.; Song, S.; Joo, K.-I.; Kim, J.; Hwang, S.H.; Jeong, J.; Kim, H. Bright, wind-driven white mechanoluminescence from zinc sulphide microparticles embedded in a polydimethylsiloxane elastomer. *Energy Environ. Sci.* **2014**, *7*, 3338–3346.
13. Zhang, J.-C.; Xu, C.-N.; Kamimura, S.; Terasawa, Y.; Yamada, H.; Wang, X. An intense elastico-mechanoluminescence material CaZnOS:Mn^{2+} for sensing and imaging multiple mechanical stresses. *Opt. Express* **2013**, *21*, 12976–12986.
14. Zhang, J.-C.; Long, Y.-Z.; Yan, X.; Wang, X.; Wang, F. Creating Recoverable Mechanoluminescence in Piezoelectric Calcium Niobates through Pr^{3+} Doping. *Chem. Mater.* **2016**, *28*, 4052–4057.
15. Zhang, J.-C.; Pan, C.; Zhu, Y.F.; Zhao, L.Z.; He, H.W.; Liu, X.; Qiu, Z. Achieving Thermo-Mechano-Opto-Responsive Bitemporal Colorful Luminescence via Multiplexing of Dual Lanthanides in Piezoelectric Particles and its Multidimensional Anticounterfeiting. *Adv. Mater*. **2018**, *30*, 1804644.
16. Kerekes, T.-W.; You, H.; Hemmatian, T.; Kim, J.; Yun, G.J. Enhancement of mechanoluminescence sensitivity of $SrAl_2O_4$: Eu^{2+}, Dy^{3+}/Epoxy composites by ultrasonic curing treatment method. *Comp. Interfaces* **2020**, 1–23, doi:10.1080/09276440.2020.1740522.
17. Zhang, Z.-J.; Ten Kate, O.M.; Delsing, A.; Dorenbos, P.; Zhao, J.-T.; Hintzenbc, H.T. Photoluminescence properties of Pr^{3+}, Sm^{3+} and Tb^{3+} doped $SrAlSi_4N_7$ and energy level locations of rare-earth ions in $SrAlSi_4N_7$. *J. Mater. Chem. C* **2014**, *2*, 7952–7959.